PULSE AND DC OPERATION LIFETIMES OF BENT-BEAM ELECTROTHERMAL ACTUATORS

Long Que, Lisa Otradovec, Andrew D. Oliver*, and Yogesh B. Gianchandani[1]

Department of Electrical and Computer Engineering, University of Wisconsin, Madison, USA
*Electromechanical Engineering Department, Sandia National Laboratories, USA

ABSTRACT

This paper reports on lifetime studies of polysilicon and p^{++} Si electrothermal actuators designed for rectilinear displacements. Measurements show that degradation patterns for displacement amplitude can be linked to design variables and operating conditions. At low power levels (which result in average operating temperatures of 300-400°C), both types of devices provide continuous DC actuation for >1400 min. and pulse actuation for >30 million cycles without change in amplitude. A model similar to that used for fatigue in steel is used to fit pulse test data for p^{++} Si actuators. The model parameters are explored as functions of operating conditions and device geometry.

I. INTRODUCTION

Electrothermal actuators have drawn increasing interest in recent years for a variety of microsystem applications. They complement electrostatic actuators by providing relatively high forces at moderate voltages, albeit at the cost of higher power dissipation [1-5]. Bent-beam electro-thermal actuators [4,5] offer rectilinear non-resonant displacements >20 μm in amplitude with forces >100 μN, drive voltages <30 V, and bandwidths >700 Hz, making them suitable for a wide variety of applications. This paper reports on studies of pulse and DC operation lifetimes of bent-beam microactuators that use polysilicon and single crystal silicon as structural materials.

Figure 1 illustrates the operating principle of a bent-beam actuator: when an electric current is passed through a V-shaped beam anchored at the two ends, thermal expansion caused by joule heating pushes the apex outward. The displacement of the apex is a function of the beam dimensions and slope, and can be increased by cascading several actuators together. As indicated in Fig. 1, the secondary units of cascaded actuators are typically not heated, although this could further amplify displacement.

The single crystal silicon devices described in this paper were fabricated by the dissolved wafer process [6], which results in heavily boron doped (p^{++}) single crystal Si structures attached to Pyrex glass substrates (Fig. 2). The glass is expansion matched to silicon, so the apex position does not drift with changes in ambient temperature. The surface micromachined polysilicon devices were fabricated on Si substrates at Sandia National Laboratories using the SUMMiT IV™ process.

The output displacements of bent-beam actuators can be predicted analytically to an accuracy of about 20% [5]. Finite element analysis (FEA) permits non-linear expansion of silicon (the expansion coefficient of which increases from 2.5 ppm/K at 20°C to 4 ppm/K at 400°C) and out-of-plane buckling limits to be taken into account. The trade-off between force and displacement is basically linear (Fig. 3). Typical responses of fabricated devices are shown in Fig. 4. The thermal isolation achieved by these devices is typically 10^3-10^4 K/W, so power consumption is <250 mW. The small thermal mass of these devices results in a relatively high bandwidth of ≈700 Hz.

II. EXPERIMENTAL RESULTS

Various designs of bent-beam and cascaded actuators were used in this study. The dimensional parameters of all devices are listed in Table I. All polysilicon and p^{++} Si devices were fabricated in single batches of wafers. The tests were performed at a probe station at 20-22°C ambient room temperature and 43-45% ambient relative humidity. Actuation amplitudes were measured by vernier scales (with a resolution of ±0.25 μm) built into the devices. Displacements that were smaller than ≈2 μm were measured by calibrated imaging for better resolution.

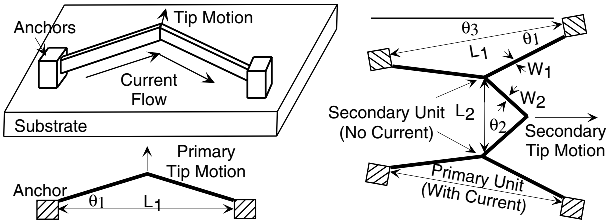

Fig. 1: Structure and operation of a single bent beam actuator (left) and cascaded design (right).

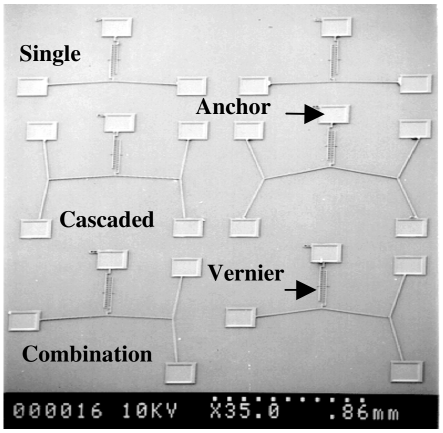

Fig. 2: SEM image of p^{++} Si electro-thermal microactuators.

The average operating temperatures of the devices were estimated from the fractional increase in the electrical resistance of the actuated bent beam. The temperature profile along a bent beam is uniform over a significant fraction of its length, but drops off in the vicinity of the anchors. The measured temperature coefficient of resistance (TCR) for p^{++} Si was 1818 ppm/K over temperatures of interest. The TCR for polysilicon was in the range of 460-600 ppm/K over the temperature range 50-150°C, and 1220 ppm/K at higher temperatures. The change in TCR for polysilicon may be

---

[1] Corresponding author: 1415 Engineering Dr., Madison, WI 53706-1691; Tel: (608) 262-2233; Fax: 262-1267; E-mail: yogesh@engr.wisc.edu

0-7803-5998-4/01/$10.00 @2001 IEEE

partially attributable to changes the grain orientation and resistivity induced by self annealing.

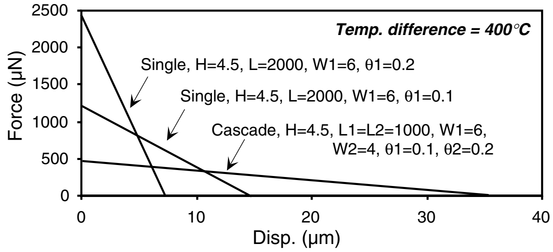

Fig. 3: FEA of tip displacement vs. loading force [4,5].

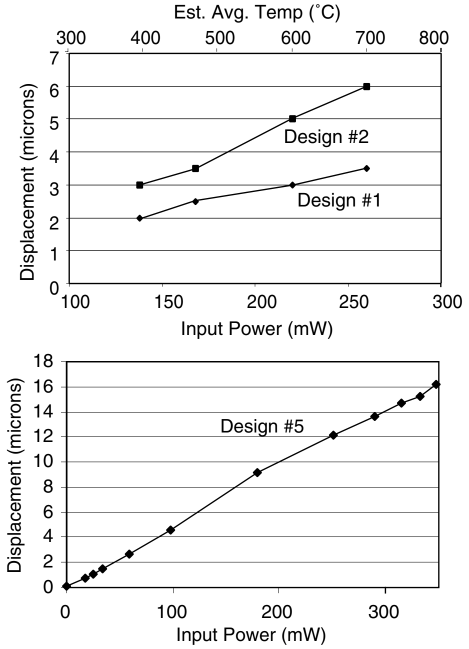

Fig. 4: Measured displacement from: (a-upper) p^{++} Si, and (b-lower) polysilicon devices. Dimensions are listed in Table I.

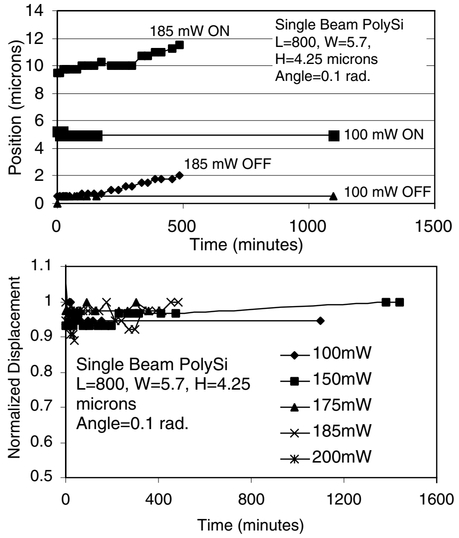

Fig. 5: (a-upper) The power-on and power-off positions increase by equal amounts over extended periods at high input power. (b-lower) The net displacement is relatively stable.

DC Tests

Actuation lifetimes were tested by applying DC power over a period of time while monitoring the location of the apex. The power was periodically turned off to monitor variations in the zero-power location of the apex. As shown in Fig. 5a, for a single beam polysilicon device (Table I, #5), actuation at 100 mW input power resulted in 5 µm displacement. A change of 0.5 µm was observed in the zero-power position of the apex after the first 10 min. of operation. However, beyond this time neither the power-off nor the power-on position changed over a cumulative actuation period of ≈1100 min. The same sample was then actuated with 185 mW input power, which resulted in a 9 µm displacement. Over the next 500 min., the power-on and power-off positions gradually increase by 2 µm, presumably because of a combination of plastic deformation and changes in the polysilicon grain structure during operation. The strain associated with these changes is calculated at –524 microstrain using the analytical approach described in [7]. It is notable that despite the change in power-on and power-off positions of the apex, the net displacement is unchanged at the end of the test period. Another polysilicon device with similar dimensions was tested at 150 mW input power. In this case the power-off and power-on positions changed by 0.5 µm in the first 75 min., but maintained a 7 µm displacement. The device was tested for a total of 1441 min., and showed no further change in the power-off position, whereas the power-on position increased by an additional 0.5 µm, resulting in a final displacement of 7.5 µm. Tests at other power levels confirmed the trends suggested by measurements already described. The normalized degradation in displacement with actuation time is shown in Fig. 5b.

A small set of p^{++} Si actuators (Table I, #1) was also subjected to DC lifetime tests. A device tested at 100 mW input power showed 4 µm net displacement with no change in power-on and power-off positions for 1500 min., at which point the test was stopped. At 180 mW input power, a net displacement of 6 µm was observed. However, the power-on and power-off positions changed by 1 µm each over a period of 90 min. Although the average and peak temperatures of p^{++} Si devices may differ from polysilicon devices tested at comparable power levels because of the different substrate materials, the qualitative similarity in observed trends suggests that some of the degradation mechanisms may be common to both types of devices. This implies that mechanisms other than grain transformations exist in polysilicon devices.

Pulse Tests

Upon repeated actuation a typical bent-beam actuator gradually degrades in amplitude. Pulse actuation studies were conducted for both polysilicon and p^{++} Si devices. The tests of polysilicon did not reveal a clear trend. However, some designs (Table I, #7) showed no indication of amplitude degradation even after 40 million cycles of 3.25 µm displacement, indicating that long lifetimes are possible at low power levels.

The p^{++} Si devices showed some interesting trends. Figure 6 shows the degradation curves for Design 2 at three different actuation temperatures. A fresh device was used for each measurement. Clearly, the degradation was more rapid at elevated temperatures, and significant reduction in amplitude is evident within the first 10 million cycles. In contrast, the cascaded device, which can be operated at lower temperatures because of the higher mechanical multiplication that it provides, showed no degradation for 30 million cycles.

The physical mechanism for amplitude degradation under repeated actuation (in which the maximum stress is below the ultimate strength of silicon) is thought to be driven by a two-part failure process: the initiation of micro-cracks and the propagation of micro-cracks in the devices. The initiation of micro-cracks mainly occurs during the boron diffusion into the silicon, and results in a dislocation density that is larger than that for weakly doped silicon [8,9]. The propagation of micro-cracks, as well as the generation of additional ones, occurs during actuation. The degradation process is expected to depend on peak stress and temperature. Therefore, when comparing devices fabricated from identical structural material, the degradation rates can be correlated to device geometry and operating temperature.

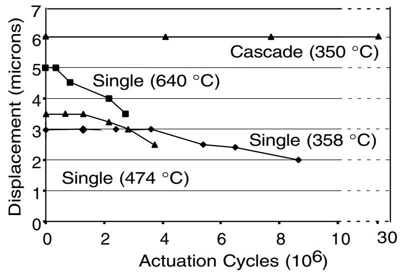

Fig. 6: Displacement degradation for the single beam Design 2 cascaded Design 4 at various temperatures.

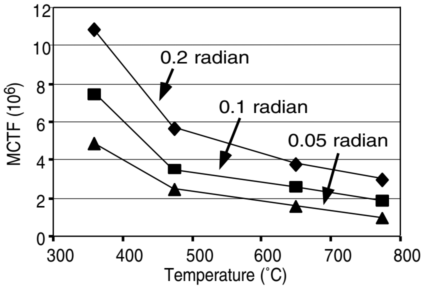

Fig.7: Mean Cycles to Failure (MCTF) observed for actuator Designs 1-3.

For the purpose of this study, the number of actuation cycles that results in an amplitude degradation of 25% in a device is labeled as its Mean Cycles to Failure (MCTF) under the specific environmental and actuation conditions that existed for the test. Figure 7 shows the MCTF of Designs 1-3 as a function of actuation temperature. Each data point in this figure represents the measurement from a single, previously unused device from a single batch of wafers. Overall, the MCTF drops from 1.1×10^7 cycles to 1.5×10^6 cycles as the operating temperature is increased from about 350°C to just under 800°C. At much higher temperatures (exceeding 1000°C), immediate plastic deformation and catastrophic failure of the actuators is observed. For most of our applications the target actuation temperature is about 450°C, and the MCTF is in the range of 3-7 million cycles for this temperature. In contrast, the cascaded device from the same wafer showed no signs of fatigue upto 30 million cycles, at which point the test was terminated. This suggests that device lifetime can be improved by >5x by selecting appropriate designs.

The inverse relationship between operating temperature and MCTF for each design in Fig. 6 is anticipated by the degradation mechanism outlined above. The measured data shows that shallower bending angles lead to a smaller MCTF at any given operating temperature. This is not surprising, because actuators with shallower bending angles experience higher stress [7]. Using FEA the peak stress at 350°C in Designs 1-3 was determined as 265 MPa, 330 MPa, and 406 MPa, respectively. (For the purpose of these simulations all devices were assumed to be 3.7 µm thick.) For the Designs 1 and 2, the peak stress occurs along the beam near the anchors, whereas for Design 3 it is near the apex. The stress at the anchor of Design 3 is 373 MPa, which is also larger than the peak stresses in Designs 1 and 2. In contrast to the simple beams, the cascaded device shows peak stress of 217 MPa midway along the beam of the secondary actuator. Although the exact stress magnitudes are moot because of the inability of the FEA to model the structural imperfections and non-uniformity in any device, the trend inversely correlates lifetime to the peak stress in these devices.

III. FAILURE MODEL

The amplitude degradation of bent-beam electro-thermal actuators under repeated operation can be empirically modeled by adapting equations that are used to predict the fatigue of steel. A study of the cyclic stability of smooth, axial specimens of steel [10] suggests that: (i) fatigue does not occur when the applied loading was below a threshold magnitude; (ii) when fatigue does occur, it has a power relation to the number of loading cycles; (iii) the cyclic degradation rate depends on loading levels. Although the criteria for applying cyclic loading and assessing fatigue in steel specimens are quite different from thermal actuators, these general observations do hold, and form the basis of an analogous mathematical model:

$$A_N = A_0 \text{ for } N \leq Ø\,(T)$$

$$A_N = A_0 \bullet K\,(\sigma(T),T) \bullet N^{-r\,(\sigma(T),T)} \text{ for } N > Ø\,(T) \qquad \ldots(1)$$

where A_N is the displacement amplitude of an actuator after N cycles, A_0 is the displacement when N=0, T is the actuation temperature, σ is the peak actuation stress in the structure, Ø is a critical value below which the degradation rate is too small to be observed, and K and r are the linear and power degradation factors, respectively. These factors are functions of actuation stress and temperature. In turn, the actuation stress depends on material properties, device geometry, and actuation temperature. For a particular structural material and device geometry, the degradation model can then be expressed as a function of temperature alone. This model is used to fit the measured data for Designs 1-3 and provides a satisfactory fit to the observed progression of failure in bent-beam actuators (Fig. 8).

It is instructive to compare the fitting parameters Ø, K, and r for Designs 1-3. The temperature dependence of these values has been separately plotted in Fig. 9-11. The offset, Ø, is consistently higher for devices with deeper bending angles at all operating temperatures, as expected. The relative longevity of the cascaded device suggests that at low stress or operating temperature the value of Ø is very large. The power factor, *r,* and the linear factor, *K,* show the same type of behavior at operating temperatures below about 600°C. However, at higher temperatures the trends are more inconsistent. This may be partially due to measurement and fitting errors, since the trend lines are close to each other at actuation temperatures above 600°C. However, it is also conceivable that self-annealing effects become significant at elevated temperatures, and they may be more prominent in devices with shallower bending angles because of the higher compressive stress in these geometries. Although most devices will not be operated at such elevated temperatures, this trend does warrant further study.

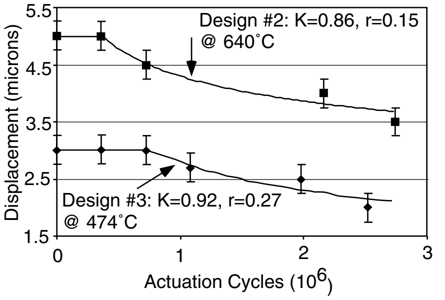

Fig. 8: A representative comparison of the degradation model in eqn. (1) to measured data for two different devices.

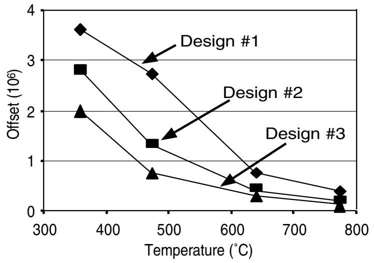

Fig. 9: The offset parameter, Ø, versus average temperature.

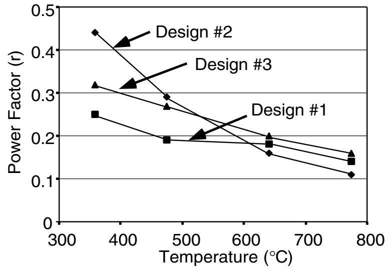

Fig. 10: The power factor, *r,* versus average temperature.

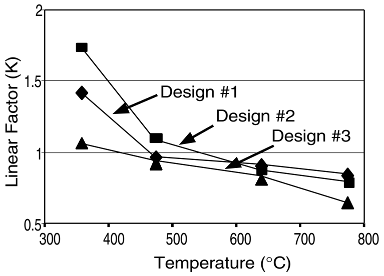

Fig. 11: The linear factor, *K,* versus average temperature.

IV. CONCLUSIONS

Long-term reliability tests of bent-beam electrothermal actuators designed for rectilinear motion and fabricated from polysilicon an p^{++} Si were conducted in laboratory ambient conditions. Measurements showed that at low power levels (which sustain average operating temperatures of 300-400°C) both types of devices provide continuous DC actuation for >1400 min. and pulse actuation for >30 million cycles without any degradation in amplitude. At higher levels of input power the power-on and power-off positions of apex are translated along the locus of motion by a few microns in a manner that suggests the accumulation of compressive stress. Despite this, the amplitude of displacement does not change. Actuation at even higher levels of input power shows increasingly rapid degradation eventually catastrophic failure of the devices. tests of the polysilicon devices did not reveal a clear trend, it was found that for the p^{++} Si devices an empirical model based on the cyclic stability of steel could fit the observed data. The fitted parameters show temperature dependence that is consistent with the physical model of the amplitude degradation, which is based on the formation and propagation of micro-cracks.

ACKNOWLEDGEMENTS

The authors thank Mr. Jae-Sung Park for assistance with the FEA and Sandia National Labs. for the fabrication of polysilicon actuators. The fabrication of p^{++} Si actuators and all measurements were performed at UW-Madison.

REFERENCES

[1] H. Guckel, J. Klein, T. Christenson, K. Skrobis, M. Laudon, E.G. Lovell, "Thermo-magnetic metal flexure actuators," *Proc., Solid-State Sensor and Actuator Workshop (Hilton Head '92),* pp. 73-75, June 1992

[2] J. Comtois, M. Michalicek, C. Barron, "Characterization of electro-thermal actuators in a…polycrystalline process," *Proc., IEEE Intl. Conf. on Solid-State Sensors and Actuators (Transducers '97),* pp. 769-772, June 1997

[3] J. Jonsmann, O. Sigmund, S. Bouwstra, "Compliant Electro-Thermal Microactuators," *IEEE Conf. on Micro Electro Mechanical Systems,* Orlando, pp. 588-592, Jan. 1999

[4] L. Que, J.-S. Park, Y.B. Gianchandani, "Bent-Beam Electro-Thermal Actuators for High Force Applications," *IEEE Conf. on Micro Electro Mechanical Systems,* Jan. '99, Orlando, FL

[5] J. Park, L. Chu, E. Siwapornsathain, A. Oliver and Y. Gianchandani, "Long throw and rotary output electro-thermal actuators based on bent-beam suspensions," *IEEE Int. Conf. on Micro Electro Mechanical Systems*, January 2000, Japan

[6] Y.B. Gianchandani, K. Najafi, "A Bulk Silicon Dissolved Wafer Process for Microelectromechanical Devices," *IEEE J. of Microelectromechanical Sys.*, 1(2), pp. 77-85, June 1992

[7] Y.B. Gianchandani, K. Najafi, "Bent-Beam Strain Sensors," *IEEE J. of Microelectromech. Sys.* 5(1), pp. 52-58, Mar. '96

[8] J. Washburn, G. Thomas, "Diffusion-induced dislocations in silicon," *J. Appl. Phys.,* 35 p. 1909, '64

[9] M. Tabib-Azar, K. Wong, Wen Ko, "Aging phenomena in heavily doped (P^+) micromachined silicon cantilever beams", *Sensors and Actuators*, A. 33 (1992), pp 199-206.

[10] R. W. Landgraf and R. A. Chernenkoff, "Residual stress effects on fatigue of surface processed steels," *Analytical and experimental methods for residual stress effects in fatigue*, Edited by Champoux, Underwood and Kapp, pp. 1-12, 1988

Table I: Dimensions of actuators (in µm) as per Fig. 1. The angle is in rad. (For design #4, θ3=0)

No.	Type	L	θ	T	W	Matl
1	Single	800	0.2	5	13.9	p^{++}Si
2	Single	800	0.1	5	13.9	p^{++}Si
3	Single	800	0.05	5	13.9	p^{++}Si
4	Casc.	800	0.2	3.7	13.9	p^{++}Si
5	Single	800	0.1	4.25	5.7	poly
6	Single	940	0.05	4.25	5.7	poly